IEEE Access
Multidisciplinary | Rapid Review | Open Access Journal

Received October 9, 2021, accepted October 30, 2021, date of publication November 8, 2021, date of current version November 18, 2021.

Digital Object Identifier 10.1109/ACCESS.2021.3126395

Long Distance Broadband Fiber Optical Beamforming Over 120 km

JICHEN QIU[1], ZHIWEI LI[1], XIAOFENG JIN[1], XIANBIN YU[1], (Senior Member, IEEE), SHILIE ZHENG[1], (Member, IEEE), AND XIANMIN ZHANG[1,2], (Member, IEEE)

[1]College of Information Science and Electronic Engineering, Zhejiang University, Hangzhou 310027, China
[2]Ningbo Research Institute, Zhejiang University, Ningbo 315100, China

Corresponding author: Xiaofeng Jin (jinxf00@zju.edu.cn)

This work was supported in part by the Natural Science Foundation of China under Grant 61871345.

ABSTRACT With the development of the space exploration and satellite communications, the data transmission at broadband and long distance are in increasing demand. To enhance the signal transmission capability from the satellite to the earth over deep space, multiple radars from distributed ground stations at cooperative mode might be a promising solution. Broadband beamforming with high efficiency over long distance fiber optic transmission links is investigated in the paper. To achieve phase stable transmission for broadband signal, fast active optical compensation is adopted by phase locking each fiber optic link with a separate wavelength to discriminate the time jitter induced phase variation. By matching the time delays between the different channels, the signal-noise ratio (SNR) of the beamformed broadband signal is improved significantly. In the experiment, a root mean square (RMS) of time delay variations of 0.86 ps and Allan deviation of 1.74×10^{-13} for the carrier transmission in the phase locked fiber link over 120 km is achieved, and broadband fiber optical beamforming with data rate over 2 Gbit/s is successfully demonstrated.

INDEX TERMS Broadband signal, optical beamforming, time jitter compensation.

I. INTRODUCTION

The evolution of satellite systems and promising space missions such as gravitational wave and black hole detection has shown a trend towards satellite communications with broader bandwidth [1]–[3]. On the one hand, the wide operating bandwidth communication means that satellites systems can provide wider communication coverage and data connections [4], [5]. On the other hand, multiple radars on the ground can also utilize a multi-channel broadband system, from which more accurate and diverse sensing information can be extracted [6]. These are of great importance for advanced satellite missions. Therefore, how to maintain the phase stability of transmission data received from radars between the different base stations over long distances and how to improve the efficiency of broadband beamforming are bottlenecks which need to be overcome [7].

The conventional implementations of high-efficiency beamforming using microwave devices such as electrical mixers, frequency multipliers as well as phase shifters, have disadvantages of limited frequency bandwidth, complex system, and sensitivity to electromagnetic interference [18]–[20]. Therefore, several optical pioneering beamforming schemes have been proposed [8]–[15]. The beamformer based on a ring resonator provides an effective way to obtain a compact and squint-free structure. In addition, the phase of modulated optical signals can be stabilized by the hybrid integration of modulators [8], [15]. However, the present photonic chips with ring resonators are suffered from the high insertion loss and the restricted operating bandwidth. Some beamformers based on ring resonators are combined with optical switches to realize wider bandwidth and continuous delay tuning [9]. Nevertheless, the main challenge is the fabrication error which limits the accuracy of the tuning increment [10]. The linearly chirped Bragg grating beamformer has been adopted to further improve the broadband capability and tuning range [11], [12]. However, the limitations of these methods based on thermal or mechanical tuning are arisen by their low switching speed of true time delay (TTD) [13]. Moreover, the stability of the system employs mechanical tuning is poor. Some beamformers employ special fibers with high dispersion and tunable light sources to achieve flexible multiple-beam transmitting and receiving [13], [14]. Although these schemes have realized large tuning scale, the system structure using multi-wavelength laser arrays seems complexed and the innate high-order dispersion obstructs the

The associate editor coordinating the review of this manuscript and approving it for publication was Joewono Widjaja.

broadband beamforming for high capacity radar signals [15]. Recently, the integrated optical beamforming networks are recognized as the promising technology in wideband systems [21], [22]. For example, a delay of 0.49 ns with a bandwidth of 10 GHz targeting X-band antenna was reported [23]. Compared with the non-integrated solutions, the integrated optical beamforming networks have much lighter weights and higher carrier frequencies [21]. However, the current integrated photonics solutions usually suffer higher insertion loss, the TTD networks as in [21]–[23] only support discrete delays and the precise control of all the switches in the network is necessary, which seems complicate.

In this letter, a scheme for broadband long distance optical beamforming is proposed and experimentally demonstrated. To achieve the phase stability of the broadband signal, the time jitter of long distance fiber is discriminated through phase locking of transmission link with a separate wavelength, and well corrected through a high-speed optical tunable delay line (OTDL). By adjusting the OTDL concurrently, the time delay matching between different channels is realized so as the signal-noise ratio (SNR) of beamforming broadband signal is significantly improved. In the experiment, a root mean square (RMS) of time delay variations of 0.86 ps and Allan deviation (ADEV) of 1.74×10^{-13} show the high stability of long distance transmission link with the applied fast active optical compensation, and broadband fiber optical beamforming over 120 km with data rate over 2 Gbit/s is also successfully demonstrated.

II. SYSTEM MODEL

Fig.1 illustrates the scheme of the long distance broadband optical beamforming link. Each optical channel link consists of a main transmission path and a phase discrimination loop. In the main transmission path, the continuous-wave (CW) light wave from a distributed feedback (DFB) laser (LD1) at the wavelength of λ_1 is sent to a Mach-Zehnder modulator (MZM1), which is driven by the corresponding remote antennas signal and biased at the quadrature point (QTP) by the bias control circuit (BC). The output of MZM1 then passes through an OTDL and a fiber link of 120 km which is composed of a section of 120 km single mode fiber (SMF) and a section of 7.8 km dispersion compensating fiber (DCF), which approximately compensating 80 km dispersion of SMF. The reason of DCF introduced here is to reduce the dispersion induced power penalty of the long fiber link. An erbium-doped fiber amplifier (EDFA) is adopted to compensate the insertion loss of the link. Using a wavelength division multiplexer (WDM3), multiple channel links modulated with wideband vector radio-frequency (RF) [16], [17] signals from different antennas at wavelength $\lambda_1 \ldots \lambda_n$ are then multiplexed and directed to a photodetector (PD1). The output electrical signal of PD1 is amplified and then monitored by an electrical spectrum analyzer (ESA).

In the phase discrimination loop, a CW light with a reference wavelength of λ_0 from another laser (LD2) is fiber-coupled into another modulator (MZM2). A RF signal

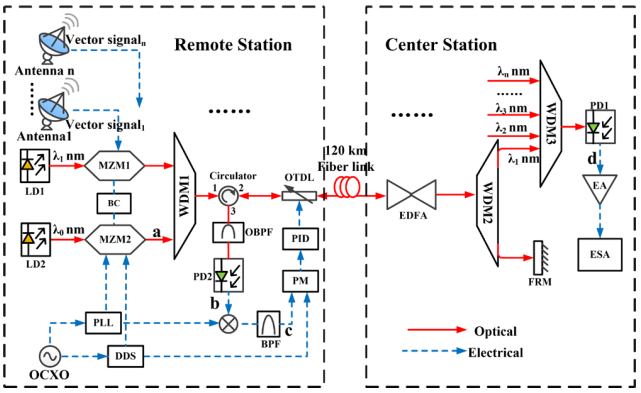

FIGURE 1. Schematic diagram of the optical broadband beamforming link over 120-km. LD: laser diode; MZM: Mach–Zehnder modulator; WDM: wavelength division multiplexer; OTDL: optical tunable delay line; EDFA: erbium-doped fiber amplifier; PD: photodetector; EA: electrical amplifier; OBPF: optical bandpass filter; BPF: bandpass filter; PM: phase discriminator; OCXO: Oven Controlled Crystal Oscillator; PID: Proportion Integral Differential; DDS: Digital Direct Synthesizer; PLL: Phase Locked Loop; BC: bias control circuit; FRM: Faraday mirror.

generated by a phase-locked loop (PLL) and a reference signal from a digital direct synthesizer (DDS) are applied to the RF port and bias port of MZM2 separately. The modulated reference light of λ_0 is multiplexed with the transmission light of λ_1 using another wavelength division multiplexer (WDM1), then passes through a circulator and double passes the same 120 km fiber link to experience the twice of phase drift induced by the fiber link, when reflected by a Faraday mirror (FRM) at the central station. The returned reference light output from the circulator is filtered by an optical bandpass filter (OBPF) centered at λ_0 and converted to an electrical signal by another photodetector (PD2). The output electrical signal of PD2 is then image-rejection mixed with the RF signal and filtered by a bandpass filter (BPF) at the center frequency of the reference signal. The phase difference between the output signal of the BPF and the reference signal is discriminated and processed by a Proportion Integral Differential (PID) regulator to control the OTDL so as to realize fast active optical compensation.

In the phase discrimination loop, assume the reference CW light of λ_0 has angular frequency ω_{c0}, the reference signal and the RF signal have the angular frequencies of ω_{IF} and ω_{LO}, and all the initial phases of these signals are zero. After frequency up-conversion in the optical domain and ignoring the high-order frequency components for simplicity, the output light waves from the MZM2 can be expressed as

$$\begin{aligned} &E_a(t) \\ &\propto \exp(j\omega_{c0}t) \cdot \cos\left[m_1 \cos(\omega_{IF}t) + m_2 \cos(\omega_{Rf}t) + \frac{\pi}{4}\right] \\ &\propto J_0(m_1) J_0(m_2) \exp(j\omega_{c0}t) + J_1(m_1) J_1(m_2) \exp(j\omega_{c0}t) \\ &\quad \cdot \cos(\omega_{IF}t + \omega_{RF}t) \\ &\quad -J_1(m_1) J_1(m_2) \exp(j\omega_{c0}t) \cdot \cos(\omega_{RF}t - \omega_{IF}t) \\ &\quad + J_0(m_1) J_1(m_2) \exp(j\omega_{c0}t) \cdot \cos(\omega_{RF}t) \\ &\quad + J_1(m_1) J_0(m_2) \exp(j\omega_{c0}t) \cdot \cos(\omega_{IF}t) \end{aligned} \quad (1)$$

where m_1 is the modulation depth of the reference signal, m_2 is the modulation index of the RF signal, J_n is the n-th order Bessel function of the first kind.

When the modulated light double passes the long fiber link, the phase of the signal is affected by the fiber link. At the output of PD2, the upper sideband electrical signal can be written as

$$V_b(t) \propto \cos\left[(\omega_{IF} + \omega_{RF})\,(t + \tau_{com} + \tau_{link})\right] \tag{2}$$

where τ_{com} is the TTD generated by OTDL, and τ_{link} is the back and forth time delay induced by the long fiber link.

When the output electrical signal of PD2 is mixed with the RF signal and filtered by BPF, the recovered signal with the phase drift of the fiber link can be expressed by

$$V_c(t) \propto \cos\left[\omega_{IF} t + (\omega_{RF} + \omega_{IF})\,(\tau_{com} + \tau_{link})\right] \tag{3}$$

The phase difference $\Delta\varphi$ between the reference signal and the recovered signal given by Eq. (3), can be written as

$$\Delta\varphi = (\omega_{RF} + \omega_{IF})\,(\tau_{com} + \tau_{link}) \tag{4}$$

Then, the phase difference $\Delta\varphi$ is integrated into a PID regulator module to control the OTDL in the link. From Eq. (4), when the $\Delta\varphi$ keeps zero or a constant by precisely and quickly adjusting the τ_{com} of OTDL, the phase variation of the transmission link can be well corrected to achieve stable phase transmission.

In the main transmission path, assume the MZM1 is modulated by a quadrature phase shift keying (QPSK) signal generated by the corresponding remote antenna, which can be represented as $\cos[\omega_s t + \theta(t)]$, where ω_s is the frequency offset of the QPSK signal, $\theta(t)$ is the modulated phase of the carrier. After the modulated optical signals at wavelength $\lambda_1 \ldots \lambda_n$ are transmitted through the long fiber link and then multiplexed by WDM3, the optical signal can be expressed by

$$E_d(t) \propto \sum_{i=1}^{n} \exp\left(j\frac{2\pi c}{\lambda_i} t\right) \cdot \cos\left[\frac{\pi}{4} + \beta_i \cos\left(\omega_s t + \theta(t) + \Delta\varphi_i\right)\right] \tag{5}$$

where β_i is the modulation depth of the transmission signal, $\Delta\varphi_i$ is the remaining phase of different channels after active compensation, and n is the number of the channels.

After being detected by PD1 and ignoring beat frequencies between different wavelengths, the power of beamforming broadband signal can be expressed by

$$I_d = \mathrm{R} \cdot E_d(t) E_d(t)^* \propto \sqrt{\sum_{i=1}^{n} V_i^2 + 2\sum_{j=1}^{n-1} V_j \sum_{p-j+1}^{n} V_p \cos\left(\Delta\varphi_j - \Delta\varphi_p\right)} \cdot \cos\left(\omega_s t + \theta(t) + \Phi\right) \tag{6}$$

where V_i represents the voltage of the modulated signal in different channels, R is the responsivity of the PD1, and Φ is a constant generated by formulas of trigonometric functions.

III. EXPERIMENTAL RESULTS AND ANALYSIS

A proof-of-concept experiment is carried out as shown in Fig. 1, and a two-channel beamforming structure is set up for the experiment. The transmission broadband signals are generated by an arbitrary waveform generator (AWG) to simulate the broadband vector signal received from the antennas, and the modulated signal power of each channel is kept at the same level. The wavelength of LD2 is 1558.1 nm, while the beamforming wavelengths λ_1, λ_2 are 1551.086 nm, 1554.08 nm, respectively. The center wavelength of the OBPF is 1558.1 nm and the bandwidth of the filter is about 0.8 nm. The EDFA with optical gain of 28 dB is used to compensate the optical loss the link. An oven controlled crystal oscillator (OCXO) with a frequency of 100 MHz is equally power-divided into two parts. The DDS receives one part of the OXCO signal to generate the reference signal of 150 MHz. And the BPF with a center frequency of 150 MHz is adopted to select the upper sideband signal with phase drift output by the mixer. The other part is used as the reference signal of PLL, which provides an output 10 GHz RF signal. The PIN photodetector PD1 is same as the PD2 in bandwidth of 12 GHz and responsivity of 0.65 A/W.

Fig. 2 shows the time delay variation of the beamforming of a single tone of 5 GHz signal generated by Keysight N9952A without and with the active optical compensation. The time delay variation without compensation has 126.8 ps within 15 minutes, which is mainly caused by the environment temperature variation. While the fast active compensation is applied in the transmission link, the RMS delay variation can be suppressed to less than 0.86 ps. The green line in Fig. 2 is a zoom view of the time delay variation with compensation. However, there is still about a ±2 ps peak-peak drift. The main reason is some sections of optical fibers used to connect lasers and WDMs are out of the compensation loop and subject to the ambient temperature change. The frequency stability of the transmitted single-tone with and

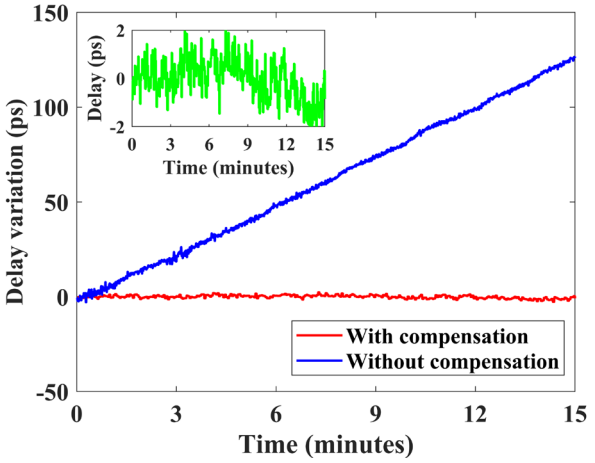

FIGURE 2. Time delay variations of the beamforming RF signal at 5 GHz over 120 km optical link without and with active compensation in 15 minutes.

without fast active compensation by overlapping ADEV and phase noise spectrum are evaluated under the same experimental conditions. As can be seen from Fig. 3, the beamforming link without compensation shows frequency drift and behaves divergence, while the overlapping ADEV of with compensation behaves convergence, reaching 1.74×10^{-13} at 1000 s. Fig. 4 shows the phase noise spectrum measured by the R&S FSW-67 ESA. Compared with the phase noise without compensation, the phase noise with compensation is averagely suppressed by 7 dB within the 4 Hz frequency offset, and the accordingly time jitter is only 0.34 ps shown in the red line. Considering a 3 dB uncertainty of the instrument, the phase noise with compensation and without compensation are almost the same as at 1 kHz to 100 kHz. In addition, it is worth noting that the spurs at 27 Hz, 1 kHz are caused by the signal generator itself. However, the compensation has little effect on the phase noise at the frequency offset beyond 4 Hz. This result shows that the bandwidth of the feedback control is about dozens of Hz, which can be improved by using the faster method of controlling the OTDL.

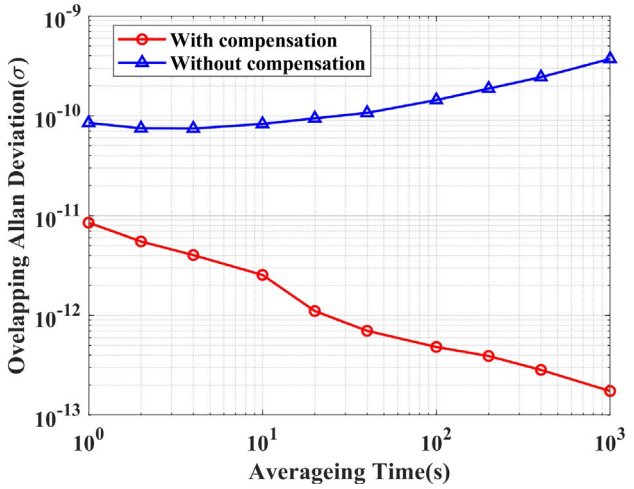

FIGURE 3. Overlapping ADEVs of the beamforming 5 GHz signal with and without phase compensation.

The beamforming signal of two-channel with a different phase difference ($\Delta\varphi_1$-$\Delta\varphi_2$) is shown experimentally. The QPSK signals with a frequency offset of 5 GHz and bits rates of 20 Mbit/s are applied to the modulators in two transmission links at the same power level. The differential delay between the two channels can be changed by adjusting the TTD of two OTDLs. The SNR of the single channel output is only about 29 dB shown by the pink line in Fig. 5. When the phase difference is 90° or 270°, it is can be seen from Eq. (6) that the output power is increased by 3 dB shown by green and blue lines in Fig. 5. When the phase difference between the two channels is nearly matched, the SNR of the beamforming signal is 35.6 dB without an electrical amplifier shown by the red line. Compared with the SNR of the single channel, the SNR of the beamforming signal can be improved by

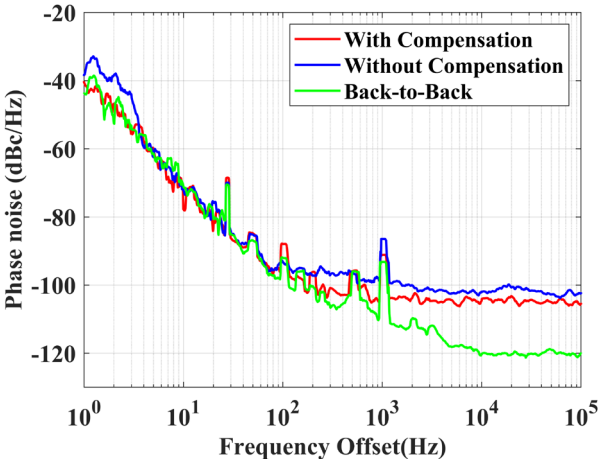

FIGURE 4. Phase noise spectrum of fiber link with compensation (red) and without compensation (blue) and back-to-back link (green).

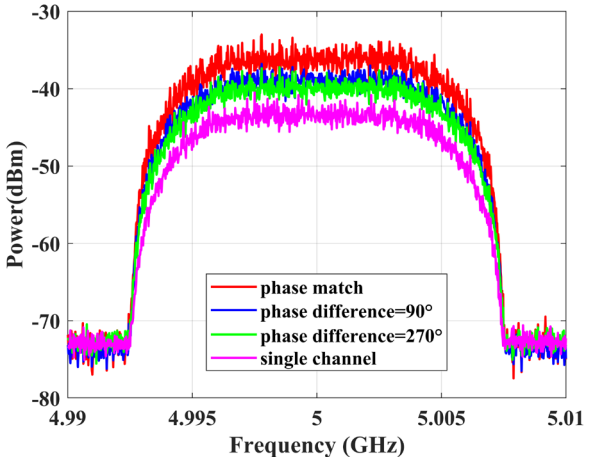

FIGURE 5. The output electrical spectrum of 5 GHz QPSK signal with symbol rates of 20 Mbit/s in the case of different phase differences between two channels.

20log2 dB by accurately delay matching between different channels.

The broadband beamforming capability of the scheme can be reflected by the maximum bits rate of the beamforming signal. Fig. 6 (a), (b) show the spectrum of 2-Gbit/s QPSK signal and 4 Gbit/s QPSK signal with a frequency offset of 5 GHz. With the help of a low noise electrical amplifier and two-channel delay match, the SNR of the 2 Gbit/s signal reaches 36.45 dB, and the SNR of the 4 Gbit/s signal is 32.72 dB. Fig. 6(c) shows the clear constellation diagram of 2 Gbit/s QPSK signal, and the error vector magnitude (EVM) is calculated to be about 12.05%. The demodulation effect of the 4 Gbit/s QPSK signal is not as good as the 2 Gbit/s QPSK signal, and the EVM is about 19.121%. Since the QPSK signal power directly generated by the AWG is relatively low, two electrical amplifiers are placed after the AWG and the PD1 to improve the output power. Slight rotations of the constellation diagram of the demodulated signal observed in

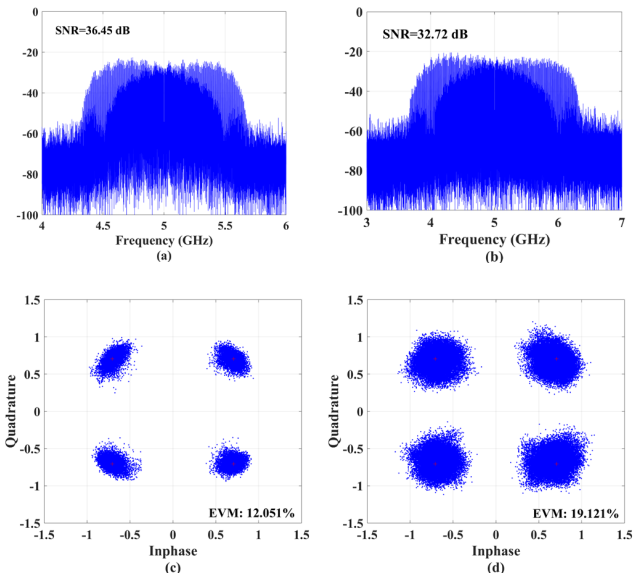

FIGURE 6. (a). Electrical spectrum of 2 Gbit/s QPSK signal with dual-channel beamforming. (b). Electrical spectrum of 4 Gbit/s QPSK signal with dual-channel beamforming. (c). The constellation diagram of 2 Gbit/s QPSK signal after demodulation. (d). The constellation diagram of 4 Gbit/s QPSK signal after demodulation.

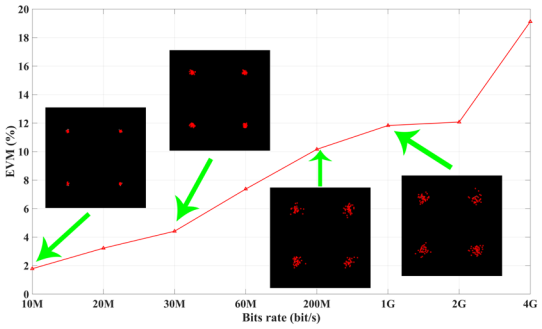

FIGURE 7. EVM results and constellation diagrams versus different baud rates of transmission signal at 5 GHz.

Fig.6 are mainly caused by the phase noise introduced by the laser diodes and the effect of dispersion of fiber link, as discussed by [24]. Fig. 7 shows the EVM results and constellation diagrams versus different baud rates of transmission signal at 5 GHz. The results show that the broadband fiber optical beamforming over 120 km with a data rate over 2-Gbit/s is successfully demonstrated.

IV. CONCLUSION

In summary, a scheme for long distance optical broadband beamforming is proposed and demonstrated. The scheme achieves phase stable transmission by phase locking to a separate wavelength with the adoption of a fast OTDL as active optical compensation. In addition, the time delay between two channels can also be matched by the OTDL so as the SNR of the beamforming signal is improved. A RMS of time delay variations of 0.86 ps and ADEV of 1.74×10^{-13} show the high stability of long distance transmission links, and broadband fiber optical beamforming over 120 km with a data rate over 2-Gbit/s is also realized experimentally. In the future, this scheme has great potential in satellite-ground communication and multiple-radar systems.

REFERENCES

[1] P. Ghelfi, F. Laghezza, F. Scotti, G. Serafino, S. Pinna, D. Onori, E. Lazzeri, and A. Bogoni, "Photonics in radar systems: RF integration for state-of-the-art functionality," *IEEE Microw. Mag.*, vol. 16, no. 8, pp. 74–83, Sep. 2015.

[2] S. Pan, D. Zhu, S. Liu, K. Xu, Y. Dai, T. Wang, J. Liu, N. Zhu, Y. Xue, and N. Liu, "Satellite payloads pay off," *IEEE Microw. Mag.*, vol. 16, no. 8, pp. 61–73, Sep. 2015.

[3] B. M. Jung and J. Yao, "A two-dimensional optical true time-delay beamformer consisting of a fiber Bragg grating prism and switch-based fiber-optic delay lines," *IEEE Photon. Technol. Lett.*, vol. 21, no. 10, pp. 627–629, May 15, 2009.

[4] M. Zhang, X. Liu, R. Pang, and G. Hu, "Two-dimensional fiber beamforming system based on mode diversity," *IEEE Access*, vol. 9, pp. 35968–35972, 2021.

[5] B. Vidal, T. Mengual, and J. Martí, "Fast optical beamforming architectures for satellite-based applications," *Adv. Opt. Technol.*, vol. 2012, pp. 1–5, Oct. 2012.

[6] B. Vidal, T. Mengual, C. Ibanez-Lopez, and J. Marti, "Optical beamforming network based on fiber-optical delay lines and spatial light modulators for large antenna arrays," *IEEE Photon. Technol. Lett.*, vol. 18, no. 24, pp. 2590–2592, Dec. 15, 2006.

[7] M. Veress, A. Barocsi, P. Richter, and P. Maak, "Theoretical and experimental analyses of the acoustic-to-optic phase transfer in specific acousto-optic devices," *Appl Opt*, vol. 49, no. 1, pp. 6–11, Jan. 1, 2010.

[8] J. Xie, L. Zhou, Z. Li, J. Wang, and J. Chen, "Seven-bit reconfigurable optical true time delay line based on silicon integration," *Opt Exp.*, vol. 22, no. 19, pp. 22707–22715, Sep. 2014.

[9] P. Zheng, C. Wang, X. Xu, J. Li, D. Lin, G. Hu, R. Zhang, B. Yun, and Y. Cui, "A seven bit silicon optical true time delay line for Ka-band phased array antenna," *IEEE Photon. J.*, vol. 11, no. 4, pp. 1–9, Aug. 2019.

[10] D. B. Hunter, M. E. Parker, and J. L. Dexter, "Demonstration of a continuously variable true-time delay beamformer using a multichannel chirped fiber grating," *IEEE Trans. Microw. Theory Techn.*, vol. 54, no. 2, pp. 861–867, Feb. 2006.

[11] H. Shahoei, M. Li, and J. Yao, "Continuously tunable time delay using an optically pumped linear chirped fiber Bragg grating," *J. Lightw. Technol.*, vol. 29, no. 10, pp. 1465–1472, May 15, 2011.

[12] H. Subbaraman, M. Y. Chen, and R. T. Chen, "Photonic crystal fiber-based true-time-delay beamformer for multiple RF beam transmission and reception of an X-band phased-array antenna," *J. Lightw. Technol.*, vol. 26, no. 15, pp. 2803–2809, Aug. 1, 2008.

[13] X. Ye, F. Zhang, and S. Pan, "Optical true time delay unit for multi-beamforming," *Opt Exp.*, vol. 23, no. 8, pp. 10002–10008, Apr. 2015.

[14] A. Meijerink, C. G. H. Roeloffzen, R. Meijerink, L. Zhuang, D. A. I. Marpaung, M. J. Bentum, M. Burla, J. Verpoorte, P. Jorna, A. Hulzinga, and W. van Etten, "Novel ring resonator-based integrated photonic beamformer for broadband phased array receive antennas—Part I: Design and performance analysis," *J. Lightw. Technol.*, vol. 28, no. 1, pp. 3–18, Jan. 1, 2010.

[15] J. Zhang and J. Yao, "Broadband microwave signal processing based on photonic dispersive delay lines," *IEEE Trans. Microw. Theory Techn.*, vol. 65, no. 5, pp. 1891–1903, May 2017.

[16] R. Kumar and S. K. Raghuwanshi, "Efficient 2D optical beamforming network with sub partitioning capability based on raised cosine chirped fiber grating and Mach-Zehnder delay interferometer," *IEEE Photon. J.*, vol. 13, no. 3, Jun. 2021, Art. no. 5500411.

[17] R. Kumar, S. K. Raghuwanshi, and D. Nadeem, "Chirped fiber grating and specialty fiber based multiwavelength optical beamforming network for 1×8 phased array antenna in S-band," *Optik*, vol. 243, Oct. 2021, Art. no. 167044.

[18] J. Zhao, D. Li, B. Ning, S. Zhang, and W. Duan, "Highly-stable frequency transfer via fiber link with improved electrical error signal extraction and compensation scheme," *Opt Exp.*, vol. 23, no. 7, pp. 8829–8836, Apr. 2015.

[19] S. Li, C. Wang, H. Lu, and J. Zhao, "Performance evaluation at the remote site for RF frequency dissemination over fiber," *IEEE Photon. J.*, vol. 9, no. 3, Jun. 2017, Art. no. 7202608.
[20] B. Ning, D. Hou, T. Zheng, and J. Zhao, "Hybrid analog-digital fiber-based radio-frequency signal distribution," *IEEE Photon. Technol. Lett.*, vol. 25, no. 16, pp. 1551–1554, Aug. 15, 2013.
[21] P. Zheng, X. Xu, D. Lin, P. Liu, G. Hu, B. Yun, and Y. Cui, "A wide-band 1×4 optical beam-forming chip based on switchable optical delay lines for Ka-band phased array," *Opt. Commun.*, vol. 488, Jun. 2021, Art. no. 126842.
[22] Y. Liu, A. Wichman, B. Isaac, J. Kalkavage, E. J. Adles, T. R. Clark, and J. Klamkin, "Tuning optimization of ring resonator delays for integrated optical beam forming networks," *J. Lightw. Technol*, vol. 35, no. 22, pp. 4954–4960, Nov. 15, 2017.
[23] C. Zhu, L. Lu, W. Shan, W. Xu, G. Zhou, L. Zhou, and J. Chen-Optica, "Silicon integrated microwave photonic beamformer," *Optica*, vol. 7, no. 9, pp. 1162–1170,2020.
[24] S. Kumar, "Effect of dispersion on nonlinear phase noise in optical transmission systems," *Opt. Lett.*, vol. 30, no. 24, pp. 3278–3280, 2005.

JICHEN QIU is currently pursuing the Ph.D. degree in electronic science and technology with the College of Information Science and Electronic Engineering, Zhejiang University. His main research interest includes microwave photonic signal processing.

ZHIWEI LI is currently pursuing the master's degree in electronics and communication engineering with Zhejiang University. His main research interests include microwave photonic sensing and signal processing.

XIAOFENG JIN received the B.S. degree in optical engineering from the Huazhong University of Science and Technology, in 1990, the Master of Engineering degree in underwater acousto-electronics engineering from the China Ship Building Institute, in 1993, and the Ph.D. degree in optical instrumentation from Zhejiang University, in 1996. He was appointed as an Associate Professor with the Department of Information and Electronic Engineering, Zhejiang University, in 1999, and promoted as a Full Professor, in 2006. His research interests include microwave photonics, photonic circuits, and smart sensing systems.

XIANBIN YU (Senior Member, IEEE) received the Ph.D. degree from Zhejiang University, Hangzhou, China, in 2005. From 2005 to 2007, he was a Postdoctoral Researcher with Tsinghua University, Beijing, China. Since November 2007, he has been with DTU Fotonik, Technical University of Denmark, Kongens Lyngby, Denmark, where he became an Assistant Professor, in 2009, and was promoted to a Senior Researcher, in 2013. He is currently a Research Professor with Zhejiang University. He has coauthored three book chapters and more than 200 peer-reviewed international journal articles and conference papers in his research interests, such as microwave photonics and optical fiber communications. His current research interests include mm-wave/THz photonics and its applications, THz communications, ultrafast photonic RF signal processing, and high-speed photonic wireless access technologies. He has given more than 30 invited international conference presentations and served as a session chair/TPC member for a number of international conferences.

SHILIE ZHENG (Member, IEEE) received the B.S. and M.S. degrees in materials science and the Ph.D. degree in physical electronics and optoelectronics from Zhejiang University, Hangzhou, China, in 1995, 1998, and 2003, respectively. In 1998, she joined the Department of Information Science and Electronic Engineering, Zhejiang University, where she was appointed as an Associate Professor, in 2005. From November 2005 to March 2006, she spent five months at Tohoku University, Japan, as a Research Assistant. From July 2016 to July 2017, she was a Visiting Research Fellow at the RF and Microwave Laboratory, National University of Singapore. At the end of 2017, she was appointed as a Full Professor with Zhejiang University. Her current research interests include twisted radio waves and applications, microwave photonics, and wireless communications.

XIANMIN ZHANG (Member, IEEE) received the B.S. and Ph.D. degrees in physical electronics and optoelectronics from Zhejiang University, Hangzhou, China, in 1987 and 1992, respectively. He was appointed as an Associate Professor of information and electronic engineering with Zhejiang University, in 1994, and a Full Professor, in 1999. He was a Research Fellow with The University of Tokyo, Tokyo, Japan, and Hokkaido University, Sapporo, Japan, from November 1996 to September 1997, and October 1997 to September 1998, respectively. In 2007, he spent two months with the Research Laboratory of Electronics, Massachusetts Institute of Technology, Cambridge, MA, USA, as a Visiting Research Fellow. He was the Dean of the Department of Information Science and Electronic Engineering, Zhejiang University, from September 2005 to November 2017, the Dean of the School of Microelectronics, Zhejiang University, from May 2015 to September 2018, the Vice Dean of the Polytechnic Institute, Zhejiang University, from July 2016 to September 2018, the President of the Ningbo Institute, Zhejiang University, from July 2018 to April 2020, and the Dean of Ningbo Campus, Zhejiang University, from September 2018 to November 2020. He is currently the Vice President of Ningbo Tech University, Ningbo, China. His research interests include microwave photonics, and electromagnetic wave theory and applications.